

Pd, Cu and bimetallic PdCu NPs supported on CNTs and phosphine-functionalized silica: one-pot preparation, characterization and testing in the semi-hydrogenation of alkynes

Daniel Sánchez-Resa,^a Jorge A. Delgado,^b Maria Dolores Fernández-Martínez,^a Chloé Didelot,^c Aimery De Mallmann,^c Kai C. Szeto,^c Mostafa Taoufik,^{*c} Carmen Claver^{a,b} and Cyril Godard,^{*a,b}

^a Departament de Química Física i Inorgànica, Universitat Rovira i Virgili, C/Marcel·lí Domingo 1, 43007 Tarragona, E-mail: cyril.godard@urv.cat

^b Centre Tecnològic de la Química, C/Marcel·lí Domingo, 43007 Tarragona.

^c C2P2, team COMS (CNRS-UMR 5265) Université Lyon 1, ESCPE Lyon 43 Boulevard du 11 Novembre 1918, 69626 Villeurbanne Cedex, France

Abstract

Triphenylphosphine stabilized Pd, Cu and PdCu nanocatalysts supported on carbon nanotubes (CNTs) or phosphorus functionalised silica (P-SiO₂) were prepared via a one-pot methodology. The series of P-SiO₂ supported catalysts evidenced metal particle sizes of metallic nanoparticles (M-NPs) between 1 and 2.4 nm, smaller than their equivalents on CNTs (2.4 – 2.6 nm). Such a difference in particle size as a function of the support and the metallic composition indicated the more pronounced mediation of the CNTs support during the formation of the M-NPs when compared to the P-SiO₂ support. The series of supported catalysts were tested in the semi-hydrogenation of alkynes providing differences in reactivity which might be correlated with the size and composition of the M-NPs and the nature of corresponding support. The carbon supported catalysts displayed in general higher activities than those supported on silica and the bimetallic catalyst PdCu/CNTs were the most selective for the case of alkyl substituted alkynes. This catalyst could moreover be recycled several times without loss of activity nor selectivity.

1. Introduction

The study of well-defined metal nanoparticles has focused much attention over the last years due to their applications in fields such as biomedicine, optical electronics, catalysis among others.^[1] Several approaches have been employed for the immobilisation of metal nanoparticles onto solid supports such as impregnation, co-precipitation or deposition,^[2] however, these methodologies often suffer from a poor control of the particle size and distribution.^[3]

In this context, surface organometallic chemistry (SOMC) offers an alternative for the preparation of well-defined heterogeneous catalysts through the grafting of organometallic species or complexes onto the surface hydroxyls of classical supports such as alumina or silica,^[4] and more recently on PNP incorporated polystyrene matrix.^[5] This methodology may also serve to selectively functionalise conventional supports with organic fragments, for example hydroquinone and triphenyl phosphine.^[6] For instance, this approach was employed for the synthesis of rhodium and platinum NPs supported on a phosphorus functionalised silica under mild conditions.^[6a] The synthesis consisted in a one-pot methodology in which the metallic precursors were reduced under H₂ atmosphere in the presence of triphenylphosphine and the phosphorus functionalised support (P-SiO₂). Under these conditions, well-dispersed small nanoparticles with an homogeneous particle size distribution (1.2 nm for Rh and 1.6 nm for Pt) were obtained.

Nanostructured carbon materials have been also employed in the last decades as carriers of metal nanoparticles, due to their special properties derived from their surface homogeneity of carbon units. This particularity has made them ideal candidates for the preparation of model catalysts adequate for systematic studies in catalysis.^[7] However, the support has not only the role of diluting or dispersing the active phase, its particular characteristics of porosity, surface chemistry, electronic environment, acidity, among others, frequently play an important role in both the synthesis of the catalyst and in the catalytic performance.^[8] For the semi-hydrogenation of alkynes, several reports have provided insights about the support dependence in catalysis.^[9] For instance, Kiwi-Minsker and co-workers reported the preparation of a composite material based on Pd nanoparticles supported on carbon nanofibers (CNF) grown on sintered metal fibers (Pd/CNF/SMF_{Inconel}).^[9b] This material was tested as nanocatalyst in the selective hydrogenation of acetylene and compared with Pd supported on activated carbon fibers (Pd/ACF). The TOF was one order of magnitude higher for Pd/CNF/SMF_{Inconel} as compared to Pd/ACF. This effect was attributed to a strong metal-support interaction of Pd⁰-nanoparticles with the graphitized CNF. According to the authors, the graphitic nature of this support could promote electron transfer between the conductive CNF and the palladium particles, thus inducing electronic perturbations of the metal then affecting the catalyst activity.

One of the strategies extensively used nowadays for enhancing the catalyst performance in the selective hydrogenation of alkynes consist in the dilution of the highly active palladium phase by a second metal with a low affinity for hydrogen (e.g. Ag, Au, Cu, etc).^[1c] The impact of such a dilution can be attributed to electronic or geometric effects.^[10] In this regard, palladium based bimetallic formulations such as PdAg,^[11] and PdAu,^[12] PdPt,^[12a] PdRhP,^[13] PdBi,^[14] PdCu^[7a, 11a, 15] among others have been reported in this reaction. In particular, bimetallic PdCu formulations have experienced special interest by the scientific community during the last years. For instance, McCue et al. reported the modification of a Cu/Al₂O₃ catalyst by various quantities of Pd precursor resulting in the formation of bimetallic catalysts with surfaces dominated by Cu.^[15a] More recently, Radivoy and co-workers reported the selective hydrogenation of terminal

alkynes, under mild reaction conditions (H_2 balloon, 110 °C), promoted by a bimetallic nanocatalyst composed of copper and palladium nanoparticles (5:1 weight ratio) supported on mesostructured silica (MCM-48).^[15b] The Cu-PdNPS@MCM-48 catalyst, which demonstrated to be highly chemoselective towards the alkyne functionality, was readily prepared from by a chemical reduction methodology using the chloride salts of Cu and Pd and Li-DTBB as the reducing agent.

In our group very recently was reported a straightforward methodology for the preparation of monometallic (copper and palladium) and bimetallic nanocatalysts (NiCu and PdCu) stabilized by a N-heterocyclic carbene ligand.^[7a] Both colloidal and supported nanoparticles (NPs) on carbon nanotubes (CNTs) were prepared via a one-pot synthesis with outstanding control on their size, morphology and composition. These catalysts were evaluated in the selective hydrogenation of alkynes and alkynols. Among the tested catalysts, PdCu/CNTs (1:1 molar ratio) revealed an efficient catalytic system providing high selectivity in the hydrogenations of terminal and internal alkynes. Moreover, this catalyst was tested in the semi-hydrogenation of acetylene in industrially relevant acetylene/ethylene-rich model gas feeds and showed excellent stability even after 40 h of reaction.

In addition to palladium based catalysts, very recently, Fedorov and co-workers reported the high potential of a non-noble metal based catalyst consisting in silica supported copper nanoparticles (capped with phosphorus or carbene ligands), in the semihydrogenation of alkynes.^[16] The authors evidenced high activity and alkene selectivity for a series of internal alkynes (at 50 bar H_2 and 60 °C) depending on the ligand used. In spite of these promising results, the preparation of well-defined metallic copper nanoparticles usually involves the use of expensive copper precursors and complicated synthetic methodologies.^[16-17] In view of the previous reports, the development of synthetic methodologies for both, copper nanoparticles and bimetallic combinations of this metal with Pd is of high interest for the semi-hydrogenation of alkynes.

In the present study, a step forward in the understanding of the reactivity in the semi-hydrogenation of alkynes of Pd, Cu and bimetallic PdCu NPs supported in different carriers is presented. To achieve this goal, two series of Pd, Cu or PdCu supported nanocatalysts were prepared on carbon nanotubes (CNTs) and phosphorus functionalized silica support (P-SiO₂), and subsequently tested in the semi-hydrogenation of alkynes. This approach permitted the identification of reactivity patterns in which the support may condition for instance the particle size of the deposited metal nanoparticles with concomitant implications in catalysis.

2. Experimental Section

A series of supported mono (Pd, Cu) and bimetallic catalysts (PdCu) were prepared in THF by reduction/decomposition of the corresponding metallic precursor(s): Mesitylcopper (I) ($CuMes$)₄, Pd(dba)₂, under hydrogen in the presence of the carrier and substoichiometric amounts of triphenylphosphine ligand.^{1b}

The following paragraphs describe the general methodology when either phosphorus functionalized silica or carbon nanotubes were employed as the carriers. For details on each synthesis see the Supporting Information.

2.1. Catalysts supported on phosphorus functionalised silica

Using a 250 ml Fischer-Porter and under nitrogen atmosphere, 150 mg of the phosphorus functionalised silica (P-SiO₂), 0.07 mmol of metallic precursor(s) (5 wt% vs. support) and 7.4 mg of PPh₃ (0.028 mmol) were dispersed in 30 ml of dry THF. The Fischer-Porter bottle was tightly closed, pressurised with 3 bars of H₂ and magnetically stirred at room temperature during 16 h. The bottle was then depressurised in air and the suspension separated by centrifugation. The supernatant was removed and the solid redispersed with *n*-hexane followed by centrifugation. The washing process was repeated 3 times and the resulting material dried under vacuum. A sample of solid was finally suspended in *n*-hexane and deposited on formvar coated copper grids for TEM analysis.

2.2. Catalysts supported on carbon nanotubes

The synthesis of carbon supported materials was analogous to the one described above (using carbon nanotubes instead of phosphorus functionalized silica), with slight differences in the work-up. After the reaction, the Fischer-Porter bottle was depressurised in air, then 30 mL of dry *n*-hexane was added and the mixture stirred for 20 min. The resulted suspension was sampled for TEM analysis. The rest was then filtered through a Nylon 66 membrane, washed with *n*-hexane and the resulting material dried in air.

2.3. General procedure for the semi-hydrogenation of alkynes

Catalytic experiments were carried out in a five-position Parr reactor provided with glass liners. In a typical experiment, the glass tube was charged with 5 mL of THF, the substrate and the corresponding amount of a previously prepared suspension of the nanocatalyst. Hydrogen gas was then introduced at the desired pressure, the magnetic stirring initiated (600 rpm) and the reactor heated at the defined temperature. After a given time, the reactor was depressurised and samples of the tubes were diluted in EtOH and analysed by GC-MS. When necessary, after the sampling, the reactor was closed and pressurised again to continue the reaction.

Recycling experiments were conducted using the PdCu/CNTs catalyst. After the first cycle (described above) the catalyst was separated by centrifugation. The supernatant was removed and analysed by GC-MS while the solid washed three times with 10 ml of cold and deoxygenated hexane, brought to dryness under reduced pressure, and later redispersed in THF. The substrate was then added for the next catalytic cycle.

3. Results and discussion

The CNTs or silica supported M-NPs were synthesised based on previously reported methods.^[6a] For each metal involved, the nominal loading was 5 wt%.

Synthesis and characterization of Pd NPs supported on CNTs and P-SiO₂

Supported Pd nanoparticles on CNTs or P-SiO₂ were prepared by decomposition of Pd(dba)₂, under 3 bar of hydrogen in the presence of triphenylphosphine (PPh₃) and carbon nanotubes (CNTs) or functionalized silica (P-SiO₂). The reaction was performed at room temperature. The solution turned black after 1 h and the catalysts were isolated by complete removal of the

solvent under vacuum. According to the TEM micrographs (Figure 1), spherical nanoparticles of *ca.* 2.5 nm and 0.9 nm were obtained when supported on CNTs and P-SiO₂ respectively.

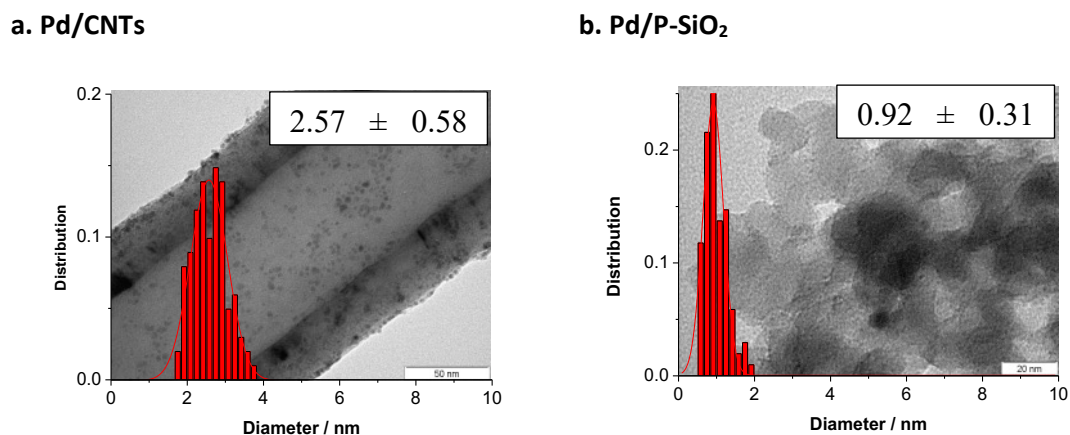


Figure 1. Size histograms and TEM micrographs of **a. Pd/CNTs** and **b. Pd/P-SiO₂**

Considering the ultra-small particle size of the NPs in **Pd/P-SiO₂**, the fine structure of this material was studied by STEM-HAADF. As appreciated in the micrograph (Figure 2), the presence of single atoms and small clusters was detected (indicated in circles) surrounding the small PdNPs. The presence of phosphorus atoms onto the support in combination with the decomposition facility of the Pd precursor might favour the deposition of single atoms or clusters onto the silica surface and the formation of ultra-small NPs. The fine structure of a single nanoparticle of *ca.* 3 nm can be also observed in Figure 2. Analysis of the electron diffraction allowed the identification of two fcc crystallographic planes, 111 and 200, which d-spacings were 2.468 and 2.192 Å, respectively. These values indicate the expansion of the crystalline lattice of the Pd NPs in **Pd/P-SiO₂** catalyst in comparison with the reference values reported for Pd-fcc (see Supporting Information). This behaviour could indicate the doping of the crystalline structure with other atoms, e.g. C or P. For instance, Asakura *et al.* reported the expansion of the crystalline lattice of PVP stabilised Pd-NPs, attributed to the presence of a palladium carbide phase (C doping) formed during the synthesis of the NPs.^[18]

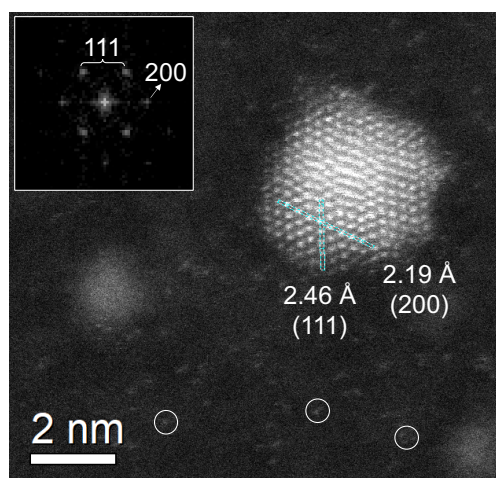


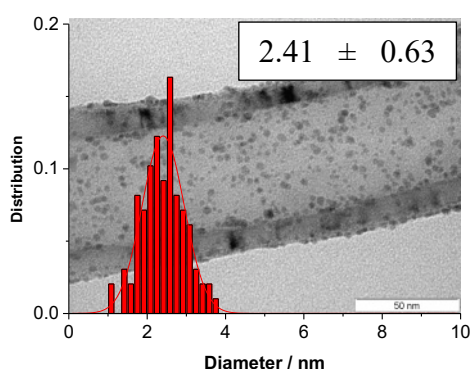
Figure 2. STEM-HAADF micrographs and electron diffraction of a nanoparticle in **Pd/P-SiO₂** catalyst. In circles several Pd single atoms and small clusters are indicated.

The crystalline structure of the synthesised materials was studied by XRD (Supporting information). A defined Pd-fcc structure was observed for **Pd/CNTs**, while the low degree of crystallinity of the **P-SiO₂** support in combination with the ultra-small size of the PdNPs did not permitted the detection of metallic diffractions. The metal loading of the prepared materials was determined by ICP. The obtained values for **Pd/CNTs** and **Pd/P-SiO₂** were both 4.4 wt%, in close agreement to the nominal value (5 wt%).

Synthesis and characterization of Cu NPs supported on CNTs and P-SiO₂

In an analogous manner, supported Cu nanoparticles on CNTs or P-SiO₂ were prepared by decomposition of (CuMes)₄ under 3 bar of hydrogen in the presence of triphenylphosphine (PPh₃) and the support. The reaction was performed at 70°C. The solution turned black after 3h h and the catalysts were isolated by complete removal of the solvent under vacuum. TEM analyses of the obtained materials revealed the formation of spherical NPs of *ca.* 2.4 and 2.1 nm for **Cu/CNTs** and **Cu/P-SiO₂** respectively (Figure 3).

a. Cu/CNTs



b. Cu/P-SiO₂

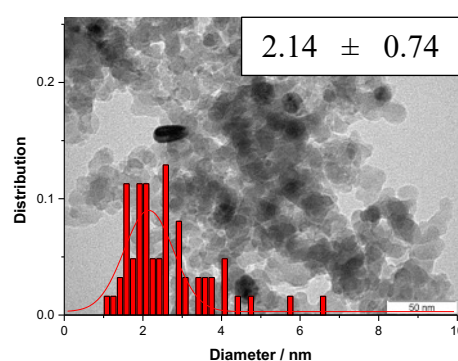


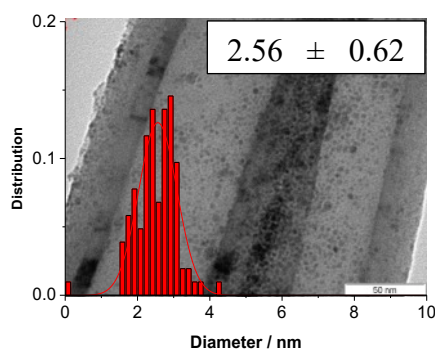
Figure 3. Size histograms and TEM micrographs of **a. Cu/CNTs** and **b. Cu/P-SiO₂**

A structural analysis of these catalysts by XRD (Supporting information) evidenced the presence of a peak at 43° assigned to the 111 plane of a Cu-fcc metallic structure. Analysis of the metal loading by ICP indicated values of 6 and 4.8 wt% for **Cu/CNTs** and **Cu/P-SiO₂** respectively.

Synthesis and characterization of PdCu NPs supported on CNTs and P-SiO₂

Bimetallic PdCu nanoparticles supported on CNTs or P-SiO₂ were prepared by decomposition of the corresponding amounts of Pd(dba)₂ and (CuMes)₄ under 3 bar of hydrogen in the presence of PPh₃ and the support (CNTs or P-SiO₂). The reaction was performed at 70°C. TEM analysis of these materials revealed the formation of PdCu NPs of *ca.* 2.6 and 1.5 nm for **PdCu/CNTs** and **PdCu/P-SiO₂** respectively (Figure 4).

a. PdCu/CNTs



b. PdCu/P-SiO₂

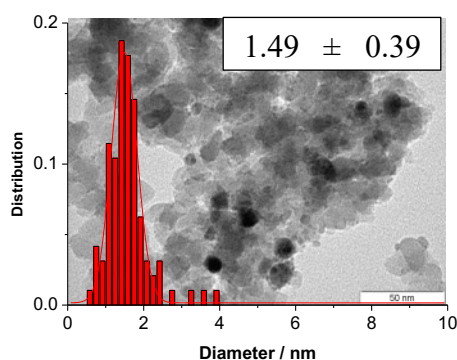


Figure 4. Size histograms and TEM micrographs of **a. PdCu/CNTs** and **b. PdCu/P-SiO₂**

The fine structure of the bimetallic catalysts was studied by STEM-HAADF. For the case of **PdCu/CNTs** (Figure 5a), fast Fourier transform (FFT) analysis of single particles permitted the identification and the measure of d-spacing corresponding to the 111 plane (2.251 Å). Microanalyses of several particles by energy dispersive X-ray spectroscopy (EDS) confirmed their bimetallic nature (Supporting Information).

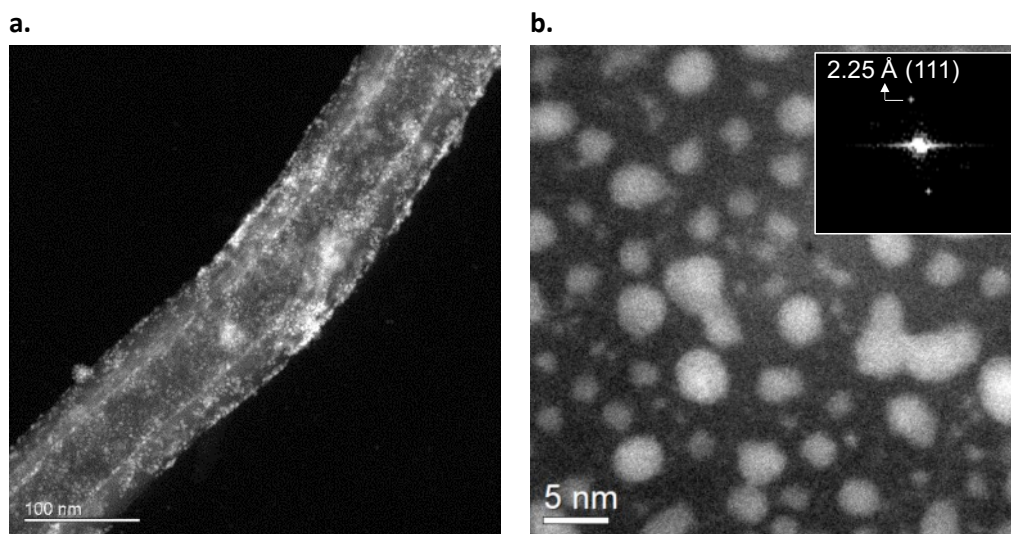


Figure 5. STEM-HAADF micrograph of bimetallic **PdCu/CNTs**. **a.** Low magnification displaying a section of CNT decorated by the NPs. **b.** High magnification; inset corresponds to a representative FFT electron diffraction of a single PdCu NP.

FFT analysis of single particles in **PdCu/P-SiO₂** (Figure 6a) permitted the identification and measurement of d-spacing of 2.410 and 2.067 Å assigned to 111 and 200 planes respectively. These values are slightly smaller when compared to those measured for Pd-NPs in **Pd/P-SiO₂** catalyst but significantly larger than reference values for Cu-fcc (2.087 and 1.808 Å for 111 and 200 planes respectively), in agreement with the formation of bimetallic PdCu nanostructures. The metal distribution in a single PdCu NP was studied by EDS of line. According to the observed profile (Figure 6b), the distribution of Pd and Cu was homogeneous along the axes, thus supporting an alloyed structure for these PdCu NPs.

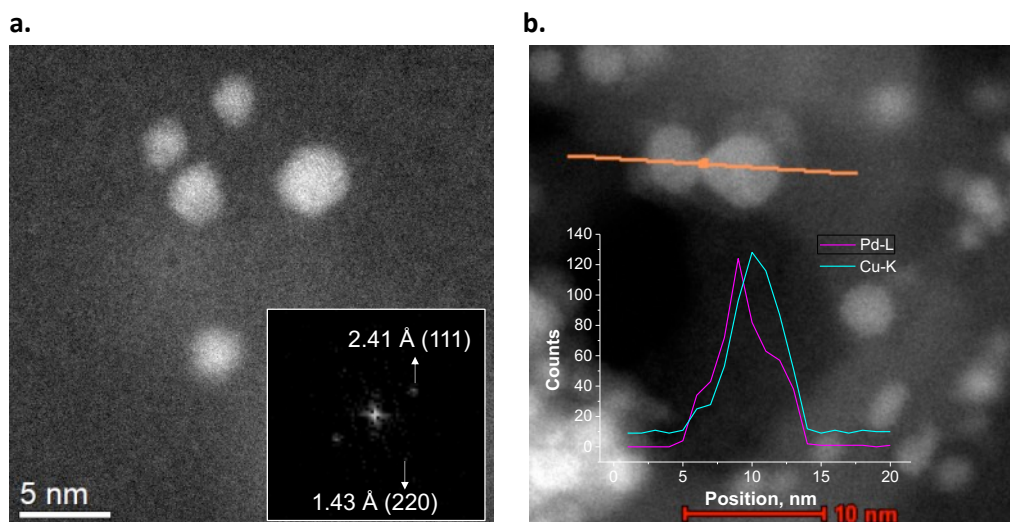


Figure 6. a. STEM-HAADF micrograph and electron diffraction (FFT) of several nanoparticles in **PdCu/P-SiO₂** catalyst. **b.** STEM-HAADF micrograph of **PdCu/P-SiO₂** catalyst; in the inset, EDX elemental analysis of line of a single PdCu particle displaying the counts distribution of Pd-L and Cu-K lines along the axes.

The XRD analysis of **PdCu/CNTs** evidenced the presence of a broad band centred at 43°, which results from the overlapping of the graphitic and metallic diffraction peaks. In contrast, for the case of **PdCu/P-SiO₂**, the signals corresponding to PdCu nanocrystals are barely distinguished from the support background due to the amorphous structure of the support in combination with the small size of the NPs. Finally, the metallic loadings measured by ICP for these two catalysts exhibited slightly negative deviations compared to the nominal value (Supporting information).

Summarizing, two main observations can be extracted from the analysis of the particles size for the series of CNTs and P-SiO₂ supported catalysts. In first place, comparing catalysts with equivalent metal compositions (e.g **Pd/CNTs** vs. **Pd/P-SiO₂**), the NPs supported on the P-SiO₂ were always smaller than their homologues on CNTs. The presence of phosphorus atoms on silica might provide additional sites for nucleation of metal clusters during the synthesis thus favouring the metal dispersion onto the support and therefore the formation of small NPs. This effect is exemplified in **Pd/P-SiO₂** where the functionalized support in combination with the decomposition facility of the Pd precursor resulted in the deposition of single atoms, clusters and ultra-small Pd NPs (of less than 1 nm) onto the silica surface. Furthermore, the fact that particle sizes on CNTs supported catalysts converged at *ca.* 2.5 nm might indicate that the CNTs possibly rules the seeding and growth of the deposited NPs independently of the metal composition. For instance, Kiwi-Minsker and co-workers reported the existence of strong metal-support interaction for a Pd catalyst supported on carbon nanofibers (CNFs) and associated it to the graphitic structure inherent to the CNFs.^[19] Differently, the particle sizes of the NPs deposited on the series of P-SiO₂ supported catalysts followed an order in agreement with the facility of decomposition/reduction of the metal formulations of each case. According to this, the particle sizes were 0.92, 1.49 and 2.14 nm for Pd, PdCu and Cu supported catalysts respectively. Considering that triphenylphosphine was added as a stabilizing agent in all the synthesis, the effect of this ligand on the particle size was discarded. Finally, the bimetallic nature and alloyed structure of the PdCu NPs in the bimetallic catalysts was evidenced.

Catalytic evaluation on the semi-hydrogenation of alkynes

In order to evaluate the reactivity of the different nanocatalysts, four model substrates with defined structural characteristics were tested. The substrates were 1-octyne, 4-octyne, phenylacetylene and diphenylacetylene.

The results of palladium catalysts are displayed in Table 1. For **Pd/CNTs** (entries 1-4), full conversion was observed except for phenylacetylene under the tested conditions. When 1-octyne was the substrate (entry 1), this catalyst displayed a high over-hydrogenation and isomerisation activity after extended reaction times (3 h). For 4-octyne (entry 2), full conversion was achieved after 0.5 h of reaction giving a 88% *cis*-selectivity which decreased to 72% after 3 h of reaction. For this substrate, the catalyst did not undergo over-hydrogenation but exhibited relevant isomerisation (16%). Regarding the aromatic substrates, for phenylacetylene (entry 3) 99% of alkene selectivity at 73% conversion was achieved after 3 h and for diphenylacetylene, full conversion was achieved at 3 h with 100% of alkene selectivity and 92% of *cis*-selectivity.

Pd/P-SiO₂ catalyst (entries 5-8), displayed lower activities in comparison to **Pd/CNTs**. When 1-octyne is employed (entry 5), 98% of alkene selectivity at 69% conversion is obtained. For 4-octyne (entry 6) full conversion was achieved with a 97% alkene selectivity and 79% of *cis*-selectivity. For the case of phenylacetylene (entry 7) a low conversion was achieved (30%) meanwhile diphenylacetylene (entry 8) exhibited 100% of alkene selectivity (90% *cis*-selectivity) at 85% conversion.

Table 1. Semi-hydrogenation of alkynes catalysed by Pd based catalysts: **Pd/CNTs** (entries 1-4) and **Pd/P-SiO₂** (entries 5-8).^a

Entry	Substrate	t, h	Conv.%	Sel. Alkene %	Sel. B %	Sel. Isomers %	<i>Cis:Trans</i>
1	1	1.5	100	92	4	4	-
		3	100	5	41	54	-
2	2	0.5	100	99	0	1	87:13
		3	100	84	0	16	72:28
3	3	3	73	99	1	0	-
4	4	3	100	100	0	0	92:8
5	1	3	70	98	0	2	-
6	2	1.5	100	97	0	3	79:21
7	3	3	30	92	8	0	-
8	4	3	85	100	0	0	90:10

^aReaction conditions: 1.35 mmol of substrate, 0.01 mol% Pd, 5 mL THF, 600 rpm, 3 bar of H₂. Entries 1-4 for **Pd/CNTs** and 5-8 for **Pd/P-SiO₂**. Conversions and selectivities were determined by GC-MS spectrometry.

The lower activities observed for **Pd/P-SiO₂** catalyst (entries 5-8) were attributed to the differences in size of the Pd NPs, (0.92 and 2.56 nm respectively), considering the well-known structure sensitivity (or particle size effect) operative in the selective hydrogenation of alkynes

and to an effect of the support (SiO₂ vs CNT).^[20] Kiwi-Minster *et al.*^[20b] studied the structure sensitivity of unsupported Pd NPs with diameters in the range 6-14 nm for the semi-hydrogenation of 1-hexyne. A progressive increase of the activity was observed when the diameter of the nanoparticles increased. The authors attributed this behaviour to the increase in the fraction of low index planes (faces) in larger NPs considering that such sites (Pd100) are more active in the hydrogenation of alkynes. Moreover, the same authors reported an increase in TOF values of one order of magnitude using palladium nanoparticles supported on carbon nanofibers grown on sintered metal fibers (CNF/SMF) rather than Pd catalyst prepared on amorphous active carbon fibers (ACF).^[19] This phenomenon was attributed to the stronger metal-support interaction of Pd-CNF/CNF due to the graphitic nature of CNF. According to the authors, electron transfer between the conductive CNF support and the palladium particles might induce electronic perturbations of the metal thus explaining the activity enhancement. Therefore, the larger particle size of the Pd NPs combined with the possible promoting effect of the CNTs could justify the observed higher activity of **Pd/CNTs** compared to **Pd/P-SiO₂**.

Next, the **PdCu/CNTs** and **PdCu/P-SiO₂** nanocatalysts were tested in the same catalytic reactions and the results are displayed in Table 2.

Table 2. Semi-hydrogenation of alkynes catalysed by bimetallic PdCu based catalysts: **PdCu/CNTs** (entries 1-4) and **PdCu/P-SiO₂** (entries 5-8).^a

(1) R₁ = (CH₂)₅CH₃; R₂ = H
 (2) R₁ = (CH₂)₂CH₃; R₂ = (CH₂)₂CH₃
 (3) R₁ = C₆H₅; R₂ = H
 (4) R₁ = C₆H₅; R₂ = C₆H₅

$$\text{R}_1\text{—}\equiv\text{—R}_2 \xrightarrow[\text{0.05\% Pd}]{\text{3 bar H}_2, \text{THF, 30 }^\circ\text{C}}$$

$\text{R}_1\text{—CH=CH—R}_2$ (cis-A) + $\text{R}_1\text{—CH=CH—R}_2$ (trans-A) + $\text{R}_1\text{—CH}_2\text{—CH—R}_2$ (B)

Entry	Substrate	t, h	Conv.%	Sel. Alkene %	Sel. B %	Sel. Isomers %	Cis:Trans
1	1	1.5	100	87	7	6	-
		3	100	74	13	13	-
2	2	0.5	100	100	0	0	92:8
		3	100	99	0	1	92:8
3	3	3	100	39	61	0	-
4	4	3	9	100	0	0	66:34
5	1	3	16	100	0	0	-
6	2	0.5	100	96	0	4	92:8
7	3	3	10	100	0	0	-
8	4	3	11	100	0	0	24:76

^aReaction conditions: 1.35 mmol of substrate, 0.05 mol% Pd (0.08 mol% Cu), 5 mL THF, 600 rpm, 3 bar of H₂. Entries 1-4 for **PdCu/CNTs** and 5-8 for **PdCu/P-SiO₂**. Conversions and selectivities were determined by GC-MS spectrometry.

When **PdCu/CNTs** were used as catalysts in the semi-hydrogenation of 1-octyne (entry 1) full conversion was obtained at 1.5 h with 87% alkene selectivity. This latter value slightly decreased to 74% after 3 h of reaction. For 4-octyne (entry 2), full conversion was achieved at 0.5 h with 100% alkene selectivity and 91% *cis*-selectivity. Interestingly, after 3 h of reaction the alkene and *cis*-selectivity remained unchanged. The low evolution of the alkene selectivity and the *cis* : *trans* ratio after extended reaction times observed for 1 and 4-octyne is an indication of the superior performance of **PdCu/CNTs** in comparison to **Pd/CNTs**. Regarding the aromatic

substrates, full conversion at 3 h was obtained for phenylacetylene (entry 3) with 61% of the over-hydrogenation product. Curiously, for diphenylacetylene (entry 4) only a 9% of conversion was achieved after 3 h.

Similar to the trend observed for the series of Pd monometallic catalysts, lower activities were obtained for **PdCu/P-SiO₂** than its analogous **PdCu/CNTs**. Conversions as low as 16% for 1-octyne (entry 5), 10% for phenylacetylene (entry 7) and 11% for diphenylacetylene (entry 8) were obtained after 3h of reaction. On the contrary, for the case of 4-octyne (entry 6) full conversion was achieved at 0.5 h with 96% alkene and 92% *cis*-selectivities. The low activity evidenced by **PdCu/P-SiO₂**, could be attributed to the ultra-small size of the PdCu NPs and the moderating effect of Cu on the activity of the active Pd phase. Conversely, the higher activity exhibited by **PdCu/CNTs** could be mainly associated to the larger particle size of the PdCu NPs.

Finally, the copper-based materials were also tested in catalysis. However no activity was observed under the tested conditions (0.7 mol% Cu, 50 °C and 3 h).

In conclusion, the introduction of Cu in the Pd structure to form a nanoalloy promotes the alkene selectivity by preventing over-hydrogenation and isomerisation processes. This observation is in agreement with a previous report where the alloying of Pd with Cu lower the hydrogenation activity and as such helps preventing overhydrogenation.^[7a] It is important to highlight, that due to the structure sensitivity of the hydrogenation of alkynes, the particle size of the M-NPs may affect the activity of a catalyst, and that the particle size is also highly influenced by the nature of the support. In this study, it was observed that CNTs favoured the formation of larger NPs which resulted in more active catalysts when compared to those prepared on P-SiO₂ which generally contained ultra-small NPs.

When a recycling experiment was performed using the **PdCu/CNTs** catalyst, the semi-hydrogenation of 4-octyne could be performed in 6 consecutive runs without loss of activity nor selectivity to the alkene product, although a slight degree of *cis/trans* isomerisation was detected after the 4th run (Figure 7).

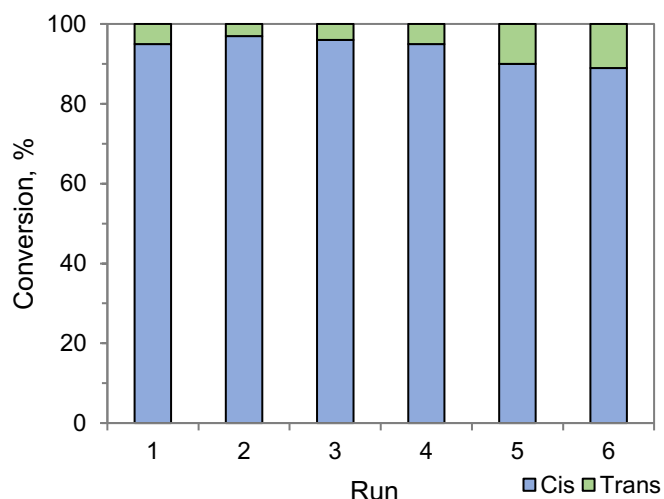


Figure 7. Recycling of **PdCu/CNTs** catalyst in the semi-hydrogenation of 4-octyne.

4. Conclusions

A general methodology was employed for the preparation of two series of supported mono (Pd and Cu) and bimetallic (PdCu) nanoparticles on carbon nanotubes and phosphorus

functionalised silica. Variations in particle size of the M-NPs as a function of the support and the metallic composition indicated a major influence of CNTs supported series. For instance, the series of CNTs catalysts evidenced in general larger particle sizes than those supported on P-SiO₂ for equivalent metallic compositions.

These materials were tested in the selective hydrogenation of alkynes giving insights into the effect of the structure of the active phase on the catalytic performance. The nanocatalysts supported on CNTs displayed a higher activity in comparison to those supported on P-SiO₂. This behaviour could be attributed to a combination of two effects: the larger particle size of the M-NPs supported on CNTs (considering that larger particles are generally more active in this reaction) and a possible electronic effect due to the graphitic nature of CNT.

In addition, the bimetallic catalyst **PdCu/CNTs** displayed a remarkable resistance against over-hydrogenation/isomerisation after full conversion of aliphatic alkynes, which is a consequence of the promoting effect of copper. These results evidence how the combination of several strategies (selection of the support, control of the particle size and the use of promoters) may result in highly structured materials with enhanced performance in catalysis.

This catalyst could moreover be recycled several times without loss of activity nor selectivity.

5. Acknowledgements

The authors acknowledge the Ministerio de Economía y Competividad and the Fondo Europeo de Desarrollo Regional FEDER (CTQ2016-75016-R, AEI/FEDER, UE, PID2019-104427RB-I00), the Generalitat de Catalunya (SGR2017) and CNRS for financial support.

Keywords: Alkyne semi-hydrogenation, Carbon nanotubes, Functionalized silica, Nanoparticles, PdCu

6. References

- [1] a) G. Schmid, in *Nanoparticles: From Theory to Applications*, Weinheim, **2010**; b) M. Diaz de los Bernardos, S. Perez-Rodriguez, A. Gual, C. Claver, C. Godard, *Chem. Commun.* **2017**, 53, 7894-7897; c) J. A. Delgado, O. Benkirane, C. Claver, D. Curulla-Ferre, C. Godard, *Dalton Trans.* **2017**, 46, 12381-12403.
- [2] a) C. J. Jia, F. Schuth, *PCCP* **2011**, 13, 2457-2487; b) M. E. Grass, Y. Zhang, D. R. Butcher, J. Y. Park, Y. Li, H. Bluhm, K. M. Bratlie, T. Zhang, G. A. Somorjai, *Angew. Chem. Int. Ed.* **2008**, 47, 8893-8896.
- [3] C. Hubert, E. G. Bile, A. Denicourt-Nowicki, A. Roucoux, *App. Catal. A Gen.* **2011**, 394, 215-219.
- [4] R. P. J. M. Basset, D. Roberto, R. Urgo, in *Modern surface organometallic chemistry*, Weinheim, **2009**.
- [5] V. Vece, K. C. Szeto, M. O. Charlin, P. Rouge, A. De Mallmann, M. Taam, P.-Y. Dugas, M. Lansalot, F. D'Agosto, M. Taoufik, *Catal. Commun.* **2019**, 129, 105715.
- [6] a) J. Llop Castelbou, K. C. Szeto, W. Barakat, N. Merle, C. Godard, M. Taoufik, C. Claver, *Chem. Commun.* **2017**, 53, 3261-3264; b) N. Popoff, J. Espinas, J. Pelletier, K. C. Szeto, J. Thivolle-Cazat, L. Delevoye, R. M. Gauvin, M. Taoufik, *ChemCatChem* **2013**, 5, 1971-1977.
- [7] a) D. A. Lomelí-Rosales, J. A. Delgado, M. Díaz de los Bernardos, S. Pérez-Rodríguez, A. Gual, C. Claver, C. Godard, *Chem. Eur. J.* **2019**, 25, 8321-8331; b) L. Montiel, J. A. Delgado, M. Novell, F. J. Andrade, C. Claver, P. Blondeau, C. Godard, *ChemCatChem* **2016**, 8, 3041-3044.

- [8] a) D. Uzio, G. Berhault, *Cat. Rev.* **2010**, *52*, 106-131; b) S. Yang, C. Cao, L. Peng, J. Zhang, B. Han, W. Song, *Chem. Commun.* **2016**, *52*, 3627-3630; c) Y. K. Gulyaeva, V. V. Kaichev, V. I. Zaikovskii, A. P. Suknev, B. S. Bal'zhinimaev, *App. Catal. A Gen.* **2015**, *506*, 197-205.
- [9] a) M. Crespo-Quesada, F. Cárdenas-Lizana, A.-L. Dessimoz, L. Kiwi-Minsker, *ACS Catal.* **2012**, *2*, 1773-1786; b) N. Semagina, M. Grasemann, N. Xanthopoulos, A. Renken, L. Kiwi-Minsker, *J. Catal.* **2007**, *251*, 213-222.
- [10] a) D. Mei, M. Neurock, C. M. Smith, *J. Catal.* **2009**, *268*, 181-195; b) M. García-Mota, J. Gómez-Díaz, G. Novell-Leruth, C. Vargas-Fuentes, L. Bellarosa, B. Bridier, J. Pérez-Ramírez, N. López, *Theor. Chem. Acc.* **2011**, *128*, 663-673; c) N. Lopez, C. Vargas-Fuentes, *Chem. Commun.* **2012**, *48*, 1379-1391; d) F. Studt, F. Abild-Pedersen, T. Bligaard, R. Z. Sørensen, C. H. Christensen, J. K. Nørskov, *Science* **2008**, *320*, 1320-1322; e) E. Vignola, S. N. Steinmann, B. D. Vandegehuchte, D. Curulla, P. Sautet, *J. Phys. Chem. C* **2016**, *120*, 26320-26327.
- [11] a) A. Yarulin, I. Yuranov, F. Cárdenas-Lizana, D. T. L. Alexander, L. Kiwi-Minsker, *App. Catal. A Gen.* **2014**, *478*, 186-193; b) C. F. Calver, P. Dash, R. W. J. Scott, *ChemCatChem* **2011**, *3*, 695-697; c) T. Mitsudome, T. Urayama, K. Yamazaki, Y. Maehara, J. Yamasaki, K. Gohara, Z. Maeno, T. Mizugaki, K. Jitsukawa, K. Kaneda, *ACS Catal.* **2016**, *6*, 666-670.
- [12] a) L. M. Bronstein, D. M. Chernyshov, I. O. Volkov, M. G. Ezernitskaya, P. M. Valetsky, V. G. Matveeva, E. M. Sulman, *J. Catal.* **2000**, *196*, 302-314; b) E. Sulman, V. Matveeva, A. Usanov, Y. Kosivtsov, G. Demidenko, L. Bronstein, D. Chernyshov, P. Valetsky, *J. Mol. Catal. A: Chem.* **1999**, *146*, 265-269; c) S. Wang, Z. Xin, X. Huang, W. Yu, S. Niu, L. Shao, *PCCP* **2017**, *19*, 6164-6168.
- [13] M. Ren, C. Li, J. Chen, M. Wei, S. Shi, *Catal. Sci. Technol.* **2014**, *4*, 1920-1924.
- [14] C. W. A. Chan, A. H. Mahadi, M. M.-J. Li, E. C. Corbos, C. Tang, G. Jones, W. C. H. Kuo, J. Cookson, C. M. Brown, P. T. Bishop, S. C. E. Tsang, *Nat. Commun.* **2014**, *5*, 5787.
- [15] a) A. J. McCue, R. T. Baker, J. A. Anderson, *Faraday Discuss.* **2016**, *188*, 499-523; b) E. Buxaderas, M. A. Volpe, G. Radivoy, *Synthesis* **2019**, *51*, 1466-1472.
- [16] a) A. Fedorov, H.-J. Liu, H.-K. Lo, C. Copéret, *J. Am. Chem. Soc.* **2016**, *138*, 16502-16507; b) N. Kaeffer, H.-J. Liu, H.-K. Lo, A. Fedorov, C. Copéret, *Chem. Sci.* **2018**, *9*, 5366-5371.
- [17] A. Shaygan Nia, S. Rana, D. Döhler, F. Jirsa, A. Meister, L. Guadagno, E. Koslowski, M. Bron, W. H. Binder, *Chem. Eur. J* **2015**, *21*, 10763-10770.
- [18] T. Ohba, H. Kubo, Y. Ohshima, Y. Makita, N. Nakamura, H. Uehara, S. Takakusagi, K. Asakura, *Bull. Chem. Soc. Jpn.* **2017**, *90*, 720-727.
- [19] P. Tribolet, L. Kiwi-Minsker, *Catal. Today* **2005**, *105*, 337-343.
- [20] a) Vanharde, R. F. Hartog, *Surf. Sci.* **1969**, *15*, 189; b) N. Semagina, A. Renken, L. Kiwi-Minsker, *J. Phys. Chem. C* **2007**, *111*, 13933-13937; c) N. Semagina, A. Renken, D. Laub, L. Kiwi-Minsker, *J. Catal.* **2007**, *246*, 308-314; d) J. Hu, Z. Zhou, R. Zhang, L. Li, Z. Cheng, *J. Mol. Catal. A Chem.* **2014**, *381*, 61-69; e) D. Teschner, E. Vass, M. Havecker, S. Zafeiratos, P. Schnoerch, H. Sauer, A. Knop-Gericke, R. Schloegl, M. Chamam, A. Wootsch, A. S. Canning, J. J. Gamman, S. D. Jackson, J. McGregor, L. F. Gladden, *J. Catal.* **2006**, *242*, 26-37; f) M. Crespo-Quesada, A. Yarulin, M. Jin, Y. Xia, L. Kiwi-Minsker, *J. Am. Chem. Soc.* **2011**, *133*, 12787-12794; g) N. Semagina, L. Kiwi-Minsker, *Catal. Lett.* **2009**, *127*, 334-338.

Graphical Abstract

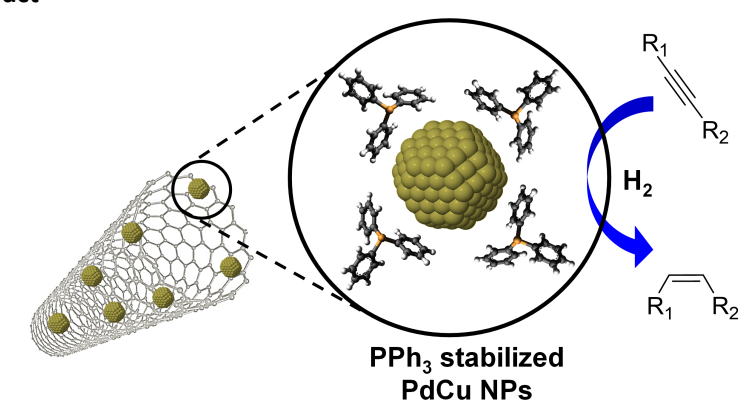


Table of contents

A one pot methodology for the preparation of triphenylphosphine stabilized Pd, Cu and PdCu nanocatalyst supported on carbon nanotubes and phosphorus functionalised silica is presented here. The catalysts were tested in the semi-hydrogenation of alkynes. Differences in reactivity were correlated with the particle size and composition of the nanoparticles and the nature of the support.